ORIGINAL RESEARCH

Evaluation of the Relationship Between the Changes in the Corneal Biomechanical Properties and Changes in the Anterior Segment OCT Parameters Following Customized Corneal Cross-Linking

Tomoya Nishida[1], Takashi Kojima [1,2], Takahiro Kataoka[1], Naoki Isogai[1], Yoko Yoshida[1], Tomoaki Nakamura [1]

[1]Nagoya Eye Clinic, Nagoya, Japan; [2]Department of Ophthalmology, Keio University School of Medicine, Tokyo, Japan

Correspondence: Takashi Kojima, Department of Ophthalmology, Keio University School of Medicine, Shinanomachi 35, Shinjuku-ku, Tokyo, Japan, Tel +81-3-5363-2012, Fax +81-3-3359-7027, Email kojkoj@me.com

Purpose: This study aimed to investigate the relationship between changes in corneal biomechanical properties and changes in anterior segment optical coherence tomography (AS-OCT) parameters preoperatively and following customized corneal cross-linking (C-CXL) in eyes with progressive keratoconus.

Patients and Methods: This study included 44 eyes of 44 patients (33 men, 11 women; average age 22.8 ± 6.4 years) who underwent C-CXL for progressive keratoconus. Scheimpflug-based tonometer (SBT) and AS-OCT findings were evaluated preoperatively and 3 months following CXL. Parameters related to changes in SBT parameters were examined by multiple regression analysis using the stepwise method.

Results: Regarding SBT parameters, significant changes were observed in the integrated area under the curve of the inverse concave radius (pre, 12.19 ± 1.95/mm; post, 11.26 ± 1.89/mm; $p < 0.0001$), maximum inverse radius (pre, 0.24 ± 0.04/mm; post, 0.23 ± 0.04/mm; $p = 0.0053$), deformation amplitude ratio max 2 mm (pre, 5.53 ± 0.81; post, 5.29 ± 0.71; $p = 0.0048$), and stress–strain index (pre, 0.74 ± 0.16; post, 0.84 ± 0.20; $p < 0.0001$), pre and post C-CXL. Regarding AS-OCT parameters, significant changes were observed in average keratometry (pre, 47.87 ± 3.61 D; post, 47.56 ± 3.29 D, $p = 0.0104$), steep keratometry (pre, 49.61 ± 4.01 D; post, 49.25 ± 3.59 D; $p = 0.0115$), maximum keratometry (pre, 55.44 ± 6.22 D; post, 54.68 ± 5.56 D; $p = 0.0061$), and thinnest corneal thickness (pre, 450.43 ± 41.74 μm; post, 444.00 ± 39.35 μm; $p < 0.0001$), pre and post C-CXL. Multiple regression analysis demonstrated that when the change in the deformation amplitude (DA) ratio max (2 mm) was the dependent variable, age, change in average keratometry, and change in the thinnest corneal thickness were selected as explanatory variables. When changes in the stiffness parameter at applanation 1 and stress–strain index were the dependent variables, change in the intraocular pressure (IOP) was selected as the explanatory variable.

Conclusion: Change in the SBT parameters following C-CXL could be related to the age, change in the IOP value, change in average keratometry, and thinnest corneal thickness.

Keywords: keratoconus, corneal biomechanics, corneal tomography, customized corneal cross-linking

Introduction

Keratoconus is a non-inflammatory corneal disease characterized by anterior protrusion, thinning of the cornea, and irregular corneal astigmatism.[1] It generally develops and progresses during puberty, resulting in irreversible loss of vision.[2] The etiology of keratoconus is unknown; however, it is associated with chronic eye rubbing, Down's syndrome, atopic disease, rigid gas permeable (RGP) contact lens wear, and Leber's congenital amaurosis.[3]

Corneal crosslinking (CXL) was introduced by Wollensak et al in 2003 as a treatment to suppress the progression of keratoconus.[4] CXL increases the rigidity of the cornea by increasing the cross-linked structure of corneal collagen by the photochemical reaction of riboflavin and long-wavelength ultraviolet light. CXL has been reported to stabilize the corneal shape in patients with keratoconus over a long period of 10 years or more, reducing the need for corneal transplantation.[5–9]

There are several surgical methods for CXL. Accelerated CXL (A-CXL) is a method that shortens the irradiation time and increases the ultraviolet (UV) irradiation intensity based on the Bunsen–Roscoe law.[10] Transepithelial corneal crosslinking, which preserves the corneal epithelium, was also developed later.[11]

A study using Brillouin microscopy showed that the cornea of patients with keratoconus had reduced biomechanical properties at the cone; however, it was near normal at the periphery.[12] Based on this observation, customized CXL (C-CXL), which irradiates UV according to the corneal shape, was developed.[13] Previous literature showed that C-CXL improved biomechanical properties and corneal shape more than A-CXL.[14] There are many reports on the effectiveness of CXL, but most of them focus on the flattening of the corneal shape. However, it is desirable to measure and evaluate the effects of CXL based on corneal biomechanical properties.[15,16] Commercially available instruments capable of measuring corneal biomechanical properties include the ocular response analyzer (ORA; Reichert Ophthalmic Instruments, Depew, NY, USA) and Scheimpflug-based tonometer (SBT; Corvis ST, Oculus, Wetzlar, Germany). These devices are also useful for diagnosing keratoconus.[17,18] In addition, numerous previous reports have demonstrated the biomechanical parameters of SBT to be reduced in keratoconus compared to that in normal corneas.[19–21]

However, while there are many facilities where corneal shape analyzers are available, few facilities are equipped with devices that can measure these biomechanical characteristics.

Therefore, in this study, we examined the extent to which the change in corneal biomechanical properties after CXL is affected by the parameters obtained from general examination equipment, such as corneal shape analyzers and conventional non-contact tonometers (NCTs). Furthermore, we examined whether these examinations could be used as substitutes for evaluation of biomechanical parameters to determine the effectiveness of CXL therapy.

Patients and Methods

Patients who underwent customized CXL for progressive keratoconus or possible keratoconus at the Nagoya Eye Clinic between January 2015 and May 2021 were retrospectively screened. Keratoconus was diagnosed by two corneal specialists (T.K and T.N).

The diagnosis of keratoconus was made by slit-lamp microscopy and corneal topography (TMS4: TOMEY). The diagnosis of keratoconus was made when slit-lamp microscopy showed Vogt's striae or Fleischer's ring or local thinning and corneal topography was positive for the Klyce/Maeda keratoconus prediction index. The diagnosis of suspected keratoconus was made based on the absence of keratoconus upon slit-lamp microscopy and only when the Klyce/Maeda keratoconus index was positive.

Anterior segment optical coherence tomography (AS-OCT; CASIA or CASIA2: TOMEY) were used. SBT was used to measure the biomechanical properties.

A non-contact tonometer (NCT; TX-F, Canon, Tokyo, Japan) was used to measure intraocular pressure (IOP). The biomechanically corrected IOP (bIOP), an intraocular pressure value considering the corneal biomechanical characteristics, was used for the intraocular pressure value obtained using SBT. Patients with ocular diseases other than refractive errors, and a history of ocular surgery other than C-CXL were excluded. In addition, individuals who wore RGP lenses on the day of the examination were excluded because the RGP lens affects the corneal shape and SBT measurement results.[22] Finally, the study enrolled 44 eyes of 44 patients (33 men, 11 women; average age 22.8±6.4 years).

This study was approved by the Nagoya Eye Clinic Ethics Committee (2021–47) and performed in accordance with the tenets of the Declaration of Helsinki. Written informed consent was waived owing to the retrospective nature of the study; however, patients were able to decline participation using an opt-out method.

Scheimpflug-Based Tonometer (SBT) Measurement

SBT blows compressed air onto the cornea and records the dynamic response of the cornea using an ultra-fast Scheimpflug camera at 4330 frames per second. The intraocular pressure value, corneal thickness, and biomechanical

characteristic values were calculated from the deformation speed and amount of corneal deformation caused by the compressed air. The following six parameters were used in this study:

Biomechanical-Corrected IOP (bIOP) (mmHg)

bIOP represents the intraocular pressure value corrected for biomechanical properties. The correction formula for calculating bIOP includes age, central corneal thickness, corneal curvature (highest concavity radius) when the cornea is maximally deformed, and 19 constants.[23]

Integrated Area Under the Curve of the Inverse Concave Radius (Integrated Radius) (1/mm)

The Integrated radius indicates the integrated value of the radius of corneal curvature when the cornea is in the most concave position after blowing of compressed air. It has been reported that the higher the corneal stiffness, the smaller the integrated radius.[24]

Maximum Inverse Radius (Max Inverse Radius) (1/mm)

The Max inverse radius shows the reciprocal of the radius of curvature of the cornea when it is in the most concave position after blowing of compressed air. It has been reported that the higher the corneal stiffness, the smaller the maximum inverse radius.[24]

Deformation Amplitude Ratio Max 2 mm (DA Ratio Max 2 mm)

DA ratio max 2 mm shows the ratio of deformation amplitude (when the cornea is in the most concave position) at a point 2 mm to the left and right from the apex of the cornea. It has been reported that the higher the corneal stiffness, the smaller the DA ratio max 2 mm.[24]

Stiffness Parameter at Applanation 1 (SP-A1)

SP-A1 shows the stiffness parameter at the first applanation state and evaluates the rigidity of the cornea. SP A1 is calculated using the following formula:

$$SP - A1 = (\text{adjusted AP1} - \text{bIOP})/A1 \text{ deflection amplitude}$$

AP1 indicates air pressure when the cornea is the first applanation status. The A1 deflection amplitude represents the movement of the corneal apex during the first applanation, which offsets eyeball movement. It has been reported that the higher the corneal rigidity, the higher the SP-A1.[25]

Stress–Strain Index (SSI)

SSI is a parameter created for evaluating corneal rigidity that does not depend on bIOP and corneal thickness but depends on age.[26,27] The higher the SSI, the higher the corneal rigidity.[28] SSI was calculated using the following formula:

$$SSI = f(a_1 + a_2C_1 + a_3C_2 + a_4C_1^2 + a_5C_1C_2 + a_6C_2^2 + a_7C_1^3 + a_8C_1^2C2 + a_9C1C_2^2 + C_2^3 + \ln (SP - HC))$$
$$C1 = CCT/545, C2 = bIOP/20,$$

ln (SP-HC) represents the natural logarithm of the stiffness parameter at the maximum concave surface of the cornea due to compressed air. a1 to a9 represent constants.

Measurement of AS-OCT

The following five parameters were used in this study for corneal shape evaluation.

Average keratometry (average K) (diopter: D): Average corneal refractive power of keratometric power at 3-mm diameter

Steep keratometry (Steep K) (D): Steep meridian corneal refractive power value of keratometric power at 3-mm diameter

Corneal astigmatism (cylinder) (D): Corneal astigmatism of keratometric power at 3-mm diameter

Maximum keratometry (Kmax) (D): Maximum keratometric power in the 10-mm diameter region

Thinnest corneal thickness (Thinnest) (μm): Thinnest corneal thickness in the 10-mm diameter region

Evaluation Items

Uncorrected (UDVA) and corrected distance visual acuity (CDVA), as well as findings of NCT, SBT, and AS-OCT were measured pre and 3 months post C-CXL. We examined the changes in each parameter pre and post C-CXL. Subsequently, the parameters related to the change in corneal biomechanical properties were examined by multiple regression analysis using the stepwise method.

The dependent variable was the change in SBT parameters (ΔSBT) pre and post C-CXL. The independent variables were the magnitude of change in the AS-OCT parameters (ΔAverage K, Δsteep K, Δcylinder, ΔKmax, and Δthinnest) pre and post C-CXL, the magnitude of change in IOP (ΔIOP) measured by general NCT, and age.

The relationship between the changes in these AS-OCT parameters and ΔSBT parameters was examined.

The Corneal Crosslinking Procedure

Transepithelial Customized Corneal Crosslinking (C-CXL)

For C-CXL, the irradiation diameter was set with reference to the corneal shape data obtained from preoperative AS-OCT. The custom UV irradiation was performed as described previously.[13] Briefly, the UV irradiation used a circular pattern with three different diameters. The diameter of the protruding region on the posterior corneal surface was determined using a posterior elevation map with 20-μm steps.

The minimum irradiation diameter was calculated by adding 1 mm to the posterior corneal protrusion area. The maximum irradiation diameter was determined as the area surrounding the protruding part of the anterior corneal surface in the keratometric map. The intermediate irradiation diameter was set to an intermediate value between the maximum and minimum diameters. Regarding the irradiation diameter and UV energy setting, the smallest irradiation diameter was irradiated for approximately 16 min and 40s with a total energy of 15 J/cm^2. The largest irradiation diameter was irradiated for 8 minutes with a total energy of 7.2 J/cm^2. The intermediate irradiation diameter was irradiated with a total energy of 10 J/cm^2 for approximately 11 min.

For C-CXL, 0.25% riboflavin, including ethylenediaminetetraacetic acid and benzalkonium chloride (ParaCel, Glaukos Corp, San Clemente, CA), was instilled every minute and allowed to react for 4 min without corneal epithelial detachment. Subsequently, 0.25% riboflavin was added every 30s for a total of 6 min. Oxygen goggles were worn before UV irradiation; using an oxygen concentration meter (New Cosmos Electric Co, Ltd, Osaka, Japan), it was confirmed that the oxygen concentration in the goggles increased to ≥90%. UV irradiation was then applied by pulse irradiation. A mosaic system (Glaukos Corp) was used for UV irradiation.

Sample Size Determination

The number of cases required in this study was calculated using the statistical analysis software G*power (version 3.1.9.3, Heinrich Heine, Dusseldorf University, Germany). The required number of cases was calculated using a two-sided test with a moderate correlation coefficient of 0.5, an α error of 0.05, and a detection power (1-β error) of 0.95. Therefore, 42 cases were required. Based on these results, 44 cases were included in this study.

Statistical Analyses

The Wilcoxon signed-rank test was performed to compare the parameters pre and post C-CXL. Spearman's rank correlation coefficient was used to examine the relationship between the following: changes in AS-OCT parameters and ΔSBT parameter pre and post C-CXL.

SPSS (ver. 24, IBM Japan, Tokyo) was used to perform the statistical analysis and multiple regression analysis. A p-value of less than 5% was considered statistically significant.

Results

Table 1 shows the patient demographics of this study.

Changes in IOP and Visual Acuity Pre and Post C-CXL (Table 2)

Post IOP (11.47±3.00 mm Hg) was significantly higher than that pre IOP (9.82±2.27 mm Hg; $p<0.0001$). Post bIOP (16.46±1.90 mm Hg) was also significantly higher than that pre bIOP (14.53±1.60 mm Hg; $p<0.0001$) (Table 2).

Post UDVA (logMAR) (0.58±0.49) was significantly improved compared to that pre UDVA (0.73±0.52; $p=0.0004$). Post CDVA (logMAR) (0.05±0.21) was not significantly different from that pre CDVA (0.12±0.26; $p=0.095$).

Comparison of SBT Parameters Pre and Post C-CXL (Table 3)

The post integrated radius (11.26±1.89/mm) was significantly lower than that pre integrated radius (12.19±1.95/mm; $p<0.0001$). The post maximum inverse radius (0.23±0.04/mm) was significantly lower than that pre maximum inverse

Table 1 Demographic Information of the Entire Patient Cohort

Parameter	
Patients (n)	44
Age (y)	22.8 ± 6.4
Sex, men/women	33/11
IOP (mmHg)	9.82 ± 2.27
bIOP (mmHg)	14.53 ± 1.60
UDVA (logMAR)	0.73 ± 0.52
CDVA (logMAR)	0.12 ± 0.26
Scheimpflug-based tonometer	
Integrated radius (1/mm)	12.19 ± 1.95
Max inverse radius (1/mm)	0.24 ± 0.04
DA ratio max (2 mm)	5.53 ± 0.81
SP-A1	71.09 ± 19.14
SSI	0.74 ± 0.16
Anterior segment OCT	
Average keratometry (D)	47.87 ± 3.61
Steep keratometry (D)	49.61 ± 4.01
Corneal astigmatism (D)	3.48 ± 1.84
Kmax (D)	55.44 ± 6.22
Thinnest corneal thickness (μm)	450.43 ± 41.74

Abbreviations: IOP, intraocular pressure; bIOP, biomechanically corrected intraocular pressure; UDVA, uncorrected distance visual acuity; CDVA, corrected distance visual acuity; Integrated radius, integrated area under the curve of the inverse concave radius; Max inverse radius, maximum inverse radius; DA ratio max, deformation amplitude ratio max 2 mm; SP-A1, stiffness parameter at applanation 1; SSI, stress-strain index; D, diopter; Kmax, maximum keratometry; OCT, optical coherence tomography.

Table 2 Comparison of the Preoperative and Postoperative CXL Intraocular Pressure Values and Uncorrected Distance Visual Acuity and Corrected Distance Visual Acuity

Parameter	Preoperative CXL	Postoperative CXL	p
IOP (mmHg)	9.82 ± 2.27	11.47 ± 3.00	<0.0001
bIOP (mmHg)	14.53 ± 1.60	16.46 ± 1.90	<0.0001
UDVA (logMAR)	0.73 ± 0.52	0.58 ± 0.49	0.0004
CDVA (logMAR)	0.12 ± 0.26	0.05 ± 0.21	0.095

Abbreviations: IOP, intraocular pressure; bIOP, biomechanically corrected intraocular pressure; UDVA, uncorrected distance visual acuity; CDVA, corrected distance visual acuity; CXL, corneal cross-linking.

Table 3 Comparison of the Preoperative and Postoperative CXL SBT Parameters

Parameter	Preoperative CXL	Postoperative CXL	p
Integrated radius (1/mm)	12.19 ± 1.95	11.26 ± 1.89	<0.0001
Max inverse radius (1/mm)	0.24 ± 0.04	0.23 ± 0.04	0.0053
DA ratio max (2 mm)	5.53 ± 0.81	5.29 ± 0.71	0.0048
SP-A1	71.09 ± 19.14	75.01 ± 17.63	0.0679
SSI	0.74 ± 0.16	0.84 ± 0.20	<0.0001

Abbreviations: Integrated radius, integrated area under the curve of the inverse concave radius; Max inverse radius, maximum inverse radius; DA ratio max, deformation amplitude ratio max 2 mm; SP-A1, stiffness parameter at applanation 1; SSI, stress-strain index; CXL, corneal cross-linking; SBT, Scheimpflug-based tonometer.

radius (0.24±0.04/mm; p=0.0053). The post DA ratio max (2 mm) (5.29±0.71) was significantly lower than that pre DA ratio max (2 mm) (5.53±0.81; p=0.0048). The post SP-A1 (75.01±17.63) was not significantly different from that pre SP-A1 (71.09±19.14; p=0.0679). The post SSI (0.84±0.20) was significantly higher than that pre SSI (0.74±0.16; p<0.0001) (Table 3).

Comparison of AS-OCT Parameters Pre and Post C-CXL (Table 4)

The post average K (47.56±3.29 D) was significantly lower than that pre average K (47.87±3.61 D; p=0.0104). The post steep K (49.25±3.59 D) was significantly lower than that pre steep K (49.61±4.01 D; p=0.0115). The post cylinder (3.38 ±1.68 D) was not significantly different from that pre cylinder (3.48±1.84 D; p=0.4921). The post Kmax (54.68±5.56 D) was significantly lower than that pre Kmax (55.44±6.22 D; p=0.0061). The post thinnest corneal thickness (444.00±39.35 μm) was significantly lower than that pre thinnest corneal thickness (450.43±41.74 μm; p<0.0001) (Table 4).

Table 4 Comparison of the Preoperative and Postoperative CXL AS-OCT Parameters

Parameter	Preoperative CXL	Postoperative CXL	p
Average keratometry (D)	47.87 ± 3.61	47.56 ± 3.29	0.0104
Steep keratometry (D)	49.61 ± 4.01	49.25 ± 3.59	0.0115
Corneal astigmatism (D)	3.48 ± 1.84	3.38 ± 1.68	0.4921
Kmax (D)	55.44 ± 6.22	54.68 ± 5.56	0.0061
Thinnest corneal thickness (μm)	450.43 ± 41.74	444.00 ± 39.35	< 0.0001

Abbreviations: D, diopter; Kmax, maximum keratometry; AS-OCT, anterior segment optical coherence tomography; CXL, corneal cross-linking.

Results of Multiple Regression Analysis with ∆SBT Parameters as Dependent Variable (Table 5)

∆Integrated radius (1/mm) and ∆Max inverse radius (1/mm) were not selected as explanatory variables in the multiple regression analysis. Age, ∆average K, and ∆thinnest were selected as explanatory variables for ∆DA ratio max (2 mm). A moderate positive correlation was found between ∆DA ratio max (2 mm) and age. (R=0.305, p=0.044) (Figure 1A). No significant correlation was found between ∆DA ratio max (2 mm) and ∆average K and ∆thinnest. (R=0.228, p=0.137) (R=−0.265, p=0.083) (Figure 1B and C). ∆IOP was selected as the explanatory variable for ∆SP-A1. A moderate positive correlation was found between ∆SP-A1 and ∆IOP. (R=0.332, p=0.028) (Figure 1D). ∆IOP was selected as the explanatory variable for ∆SSI. A moderate positive correlation was found between ∆SSI and ∆IOP. (R=0.308, p=0.042) (Figure 1E) (Table 5).

Relationship Between the Changes of the AS-OCT Parameters and ∆SBT Parameters

No significant correlation was found between the changes in the AS-OCT parameters and ∆integrated radius [∆average K: R=0.071, p=0.648 (Figure 2A); ∆steep K: R=0.147, p=0.342 (Figure 2B); ∆cylinder: R=0.117, p=0.449 (Figure 2C); ∆Kmax: R=0.180, p=0.242 (Figure 2D); ∆thinnest: R=−0.138, p=0.370 (Figure 2E)]. No significant correlation was found between the changes in the AS-OCT parameters and ∆Max inverse radius [∆average K: R=0.027, p=0.863 (Figure 3A); ∆steep K: R=0.029, p=0.854 (Figure 3B); ∆cylinder: R=0.017, p=0.912 (Figure 3C); ∆Kmax: R=0.025, p=0.872 (Figure 3D); ∆thinnest: R=−0.147, p=0.340 (Figure 3E)]. No significant correlation was found between the changes in the AS-OCT parameters and ∆DA ratio max (2 mm) [∆average K: R=0.228, p=0.137 (Figure 4A); ∆steep K: R=0.196, p=0.201 (Figure 4B); ∆cylinder: R=0.075, p=0.628 (Figure 4C); ∆Kmax: R=0.216, p=0.159 (Figure 4D); ∆thinnest: R=−0.265, p=0.083 (Figure 4E)]. No significant correlation was found between the changes in the AS-OCT parameters and ∆SP-A1 [∆average K: R=−0.030, p=0.848 (Figure 5A); ∆steep K: R=−0.038, p=0.805 (Figure 5B); ∆cylinder: R=−0.018, p=0.905 (Figure 5C); ∆Kmax: R=−0.028, p=0.858 (Figure 5D); ∆thinnest: R=0.47, p=0.762 (Figure 5E)]. No significant correlation was found between the changes in the AS-OCT parameters and ∆SSI [∆average K: R=−0.036, p=0.818 (Figure 6A); ∆steep K: R=−0.022, p=0.888 (Figure 6B); ∆cylinder: R=−0.017, p=0.913 (Figure 6C); ∆Kmax: R=−0.111, p=0.474 (Figure 6D); ∆thinnest: R=0.38, p=0.806 (Figure 6E)].

Table 5 Multiple Regression Analysis Investigating Factors Affecting the Changes in the Preoperative and Postoperative CXL SBT Parameters

Dependent Variable	Explanatory Variables	Partial Regression Coefficient	Standardized Partial Regression Coefficient	VIF	Coefficient of Determination (R^2)
∆Integrated radius (1/mm)	None				
∆Max inverse radius (1/mm)	None				
∆DA Ratio Max (2 mm)	Age	0.032	0.407	1.040	0.327
	∆average K (D)	0.247	0.348	1.044	
	∆thinnest (µm)	−0.015	−0.292	1.004	
∆SP-A1	∆IOP (mmHg)	1.794	0.338	1.000	0.115
∆SSI	∆IOP (mmHg)	0.022	0.363	1.000	0.132

Abbreviations: VIF, variance inflation factor; Integrated radius, integrated area under the curve of the inverse concave radius; Max inverse radius, maximum inverse radius; DA ratio max, deformation amplitude ratio max 2 mm; SP-A1, stiffness parameter at applanation 1; SSI, stress-strain index; D, diopter; average K, Average keratometry; thinnest, Thinnest corneal thickness; IOP, intraocular pressure; CXL, corneal cross-linking; SBT, Scheimpflug-based tonometer.
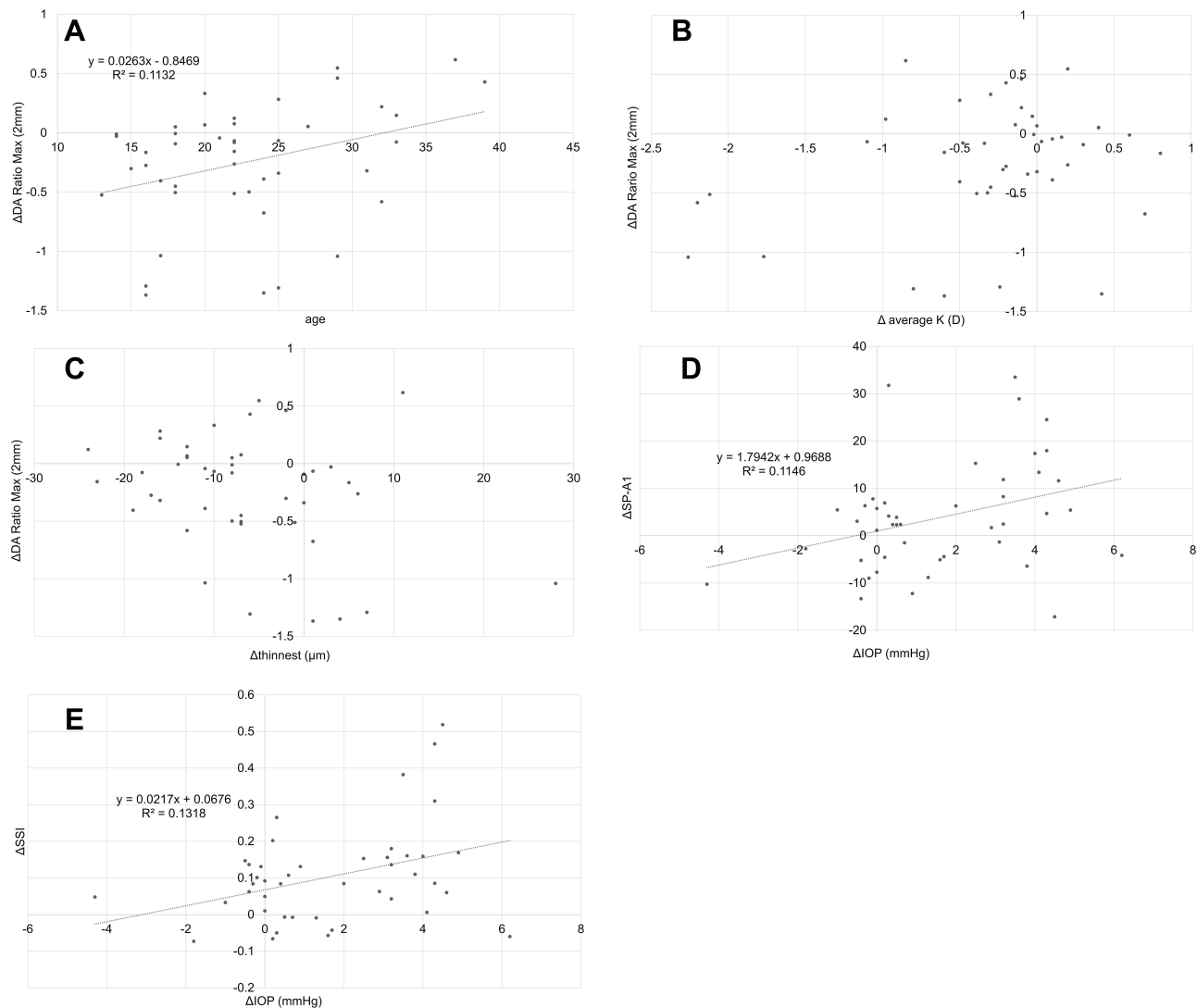
Figure 1 Correlation between Δcorneal biomechanical parameters and other parameters. A moderate positive correlation was found between the Δdeformation amplitude (DA) ratio max (2 mm) and age (**A**) (R=0.305, p=0.044). No significant correlation was found between the ΔDA Ratio Max (2 mm) and Δaverage K (**B**) (R=0.228, p=0.137). No significant correlation was found between the ΔDA Ratio Max (2 mm) and Δthinnest (**C**) (R=−0.265, p=0.083). A moderate positive correlation was found between the Δstiffness parameter at applanation 1 (SP-A1) and Δintraocular pressure (IOP) (**D**) (R=0.332, p=0.028). A moderate positive correlation was found between the Δstress-strain index (SSI) and ΔIOP (**E**) (R=0.308, p=0.042).

Discussion

It is important to assess the effectiveness of CXL treatment. As CXL increases corneal stiffness, it is reasonable to evaluate it using a corneal biomechanical property-measuring device. However, such testing instruments are only available in research institutes or core hospitals and cannot be tested everywhere. Therefore, we designed this study to examine whether the change in corneal stiffness due to C-CXL is reflected in the parameters obtained from the corneal shape analyzer, which is a widely used ophthalmic examination device.

In the current study, an increase in IOP and corneal biomechanical characteristics, particularly SSI, was observed after C-CXL. Furthermore, the corneal shape flattened after C-CXL. This change was similar to the previously reported change in Kmax at 3 months after CXL.[29]

Multiple regression analysis showed that age, Δaverage K, and Δthinnest were selected as parameters influencing ΔDA ratio max (2 mm). Among these, age had the highest influence. DA ratio max (2 mm) is
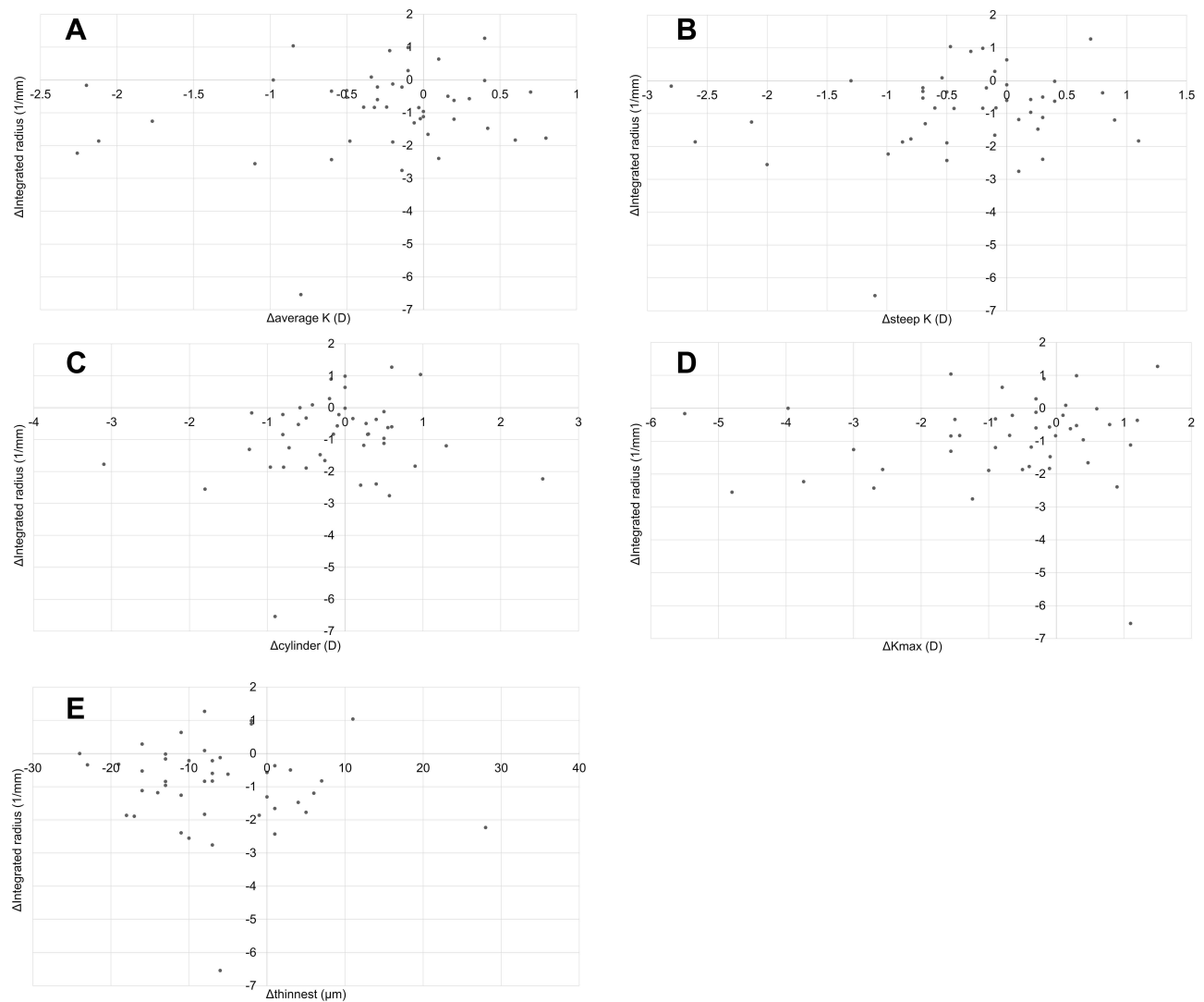
Figure 2 Correlation between each anterior segment optical coherence tomography (AS-OCT) parameter change and Δintegrated radius. No significant correlation was found between the change in each AS-OCT parameter and Δintegrated radius. ((**A**) Δaverage K, R=0.071, p=0.648) ((**B**) Δsteep K, R=0.147, p=0.342) ((**C**) Δcylinder, R=0.117, p=0.449) ((**D**) Δmaximum keratometry [Kmax], R=0.180, p=0.242) ((**E**) Δthinnest, R=−0.138, p=0.370).

a parameter that indicates that the lower the postoperative value, the greater the corneal stiffness. Therefore, the results of the standardized coefficients indicated that the younger the patient, the greater the corneal stiffness following C-CXL.

Considering the age and CXL effectiveness, some studies reported that younger age was more effective, while others reported that older age was more effective.[30,31] However, these reports used the conventional Dresden CXL method, which differs from the surgical method used in this study. In addition, the evaluation of CXL efficacy was evaluated based on the postoperative corneal shape, and there was no evaluation of the corneal biomechanical properties.

Further studies are needed concerning the relationship between the age and CXL effect in a larger number of cases. Regarding the average K, the standardized coefficient results showed that the flatter the cornea after CXL surgery, the higher the corneal stiffness. For Thinnest, the standardized coefficient results showed that the thinner the cornea after CXL surgery, the lower the corneal stiffness.
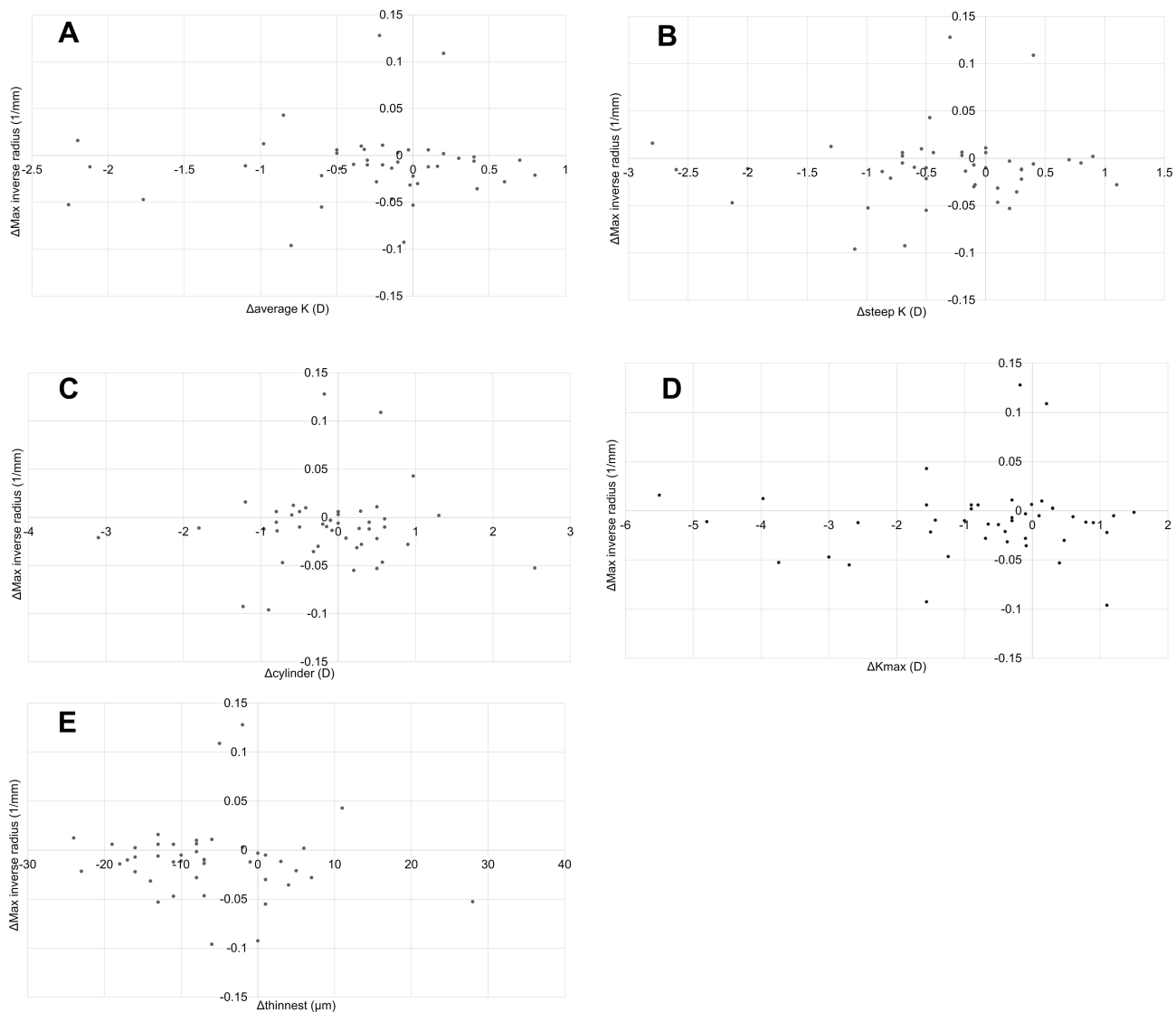
Figure 3 Correlation between each anterior segment optical coherence tomography (AS-OCT) parameter change and Δ maximum (Max) inverse radius. No significant correlation was found between the change in each AS-OCT parameter and ΔMax inverse radius. ((**A**) Δaverage K, R=0.027, p=0.863) ((**B**) Δsteep K, R=0.029, p=0.854) ((**C**) Δcylinder, R=0.017, p=0.912) ((**D**) Δ maximum keratometry [Kmax], R=0.025, p=0.872) ((**E**) Δthinnest, R=−0.147, p=0.340).

Various reports have shown that Kmax decreases after CXL.[32–35] In our study, we initially hypothesized that the flattening of Kmax after CXL reflected the effect of CXL. However, the results showed that the parameter associated with corneal stiffness was average K. One possible reason for this is the difference in the measurement point between SBT and average K. SBT measures only the horizontal corneal cross section and not the lower part of the cornea. On the other hand, average K is measured using the corneal curvature at the φ1.5 mm apart from the corneal center. In addition, multiple regression analysis selected ΔIOP as the parameter influencing ΔSP-A1 and ΔSSI.

IOP is underestimated in cases of a large corneal radius of curvature, a thin corneal thickness, and poor corneal biomechanical properties.[36] It is most affected by corneal biomechanical properties.[36] It has also been reported that post-CXL IOP measurements may be higher than preoperative IOP measurements owing to improved corneal biomechanical properties.[37] In this study, although the corneal thickness became thinner after C-CXL, an increase in IOP was observed. These results suggest that IOP was strongly influenced by the increase in corneal biomechanical properties, consistent with a previous report.[37] A positive correlation was observed between ΔSP-A1 and ΔSSI and ΔIOP, suggesting that the greater the IOP increase after CXL, the greater the improvement in biomechanical properties.
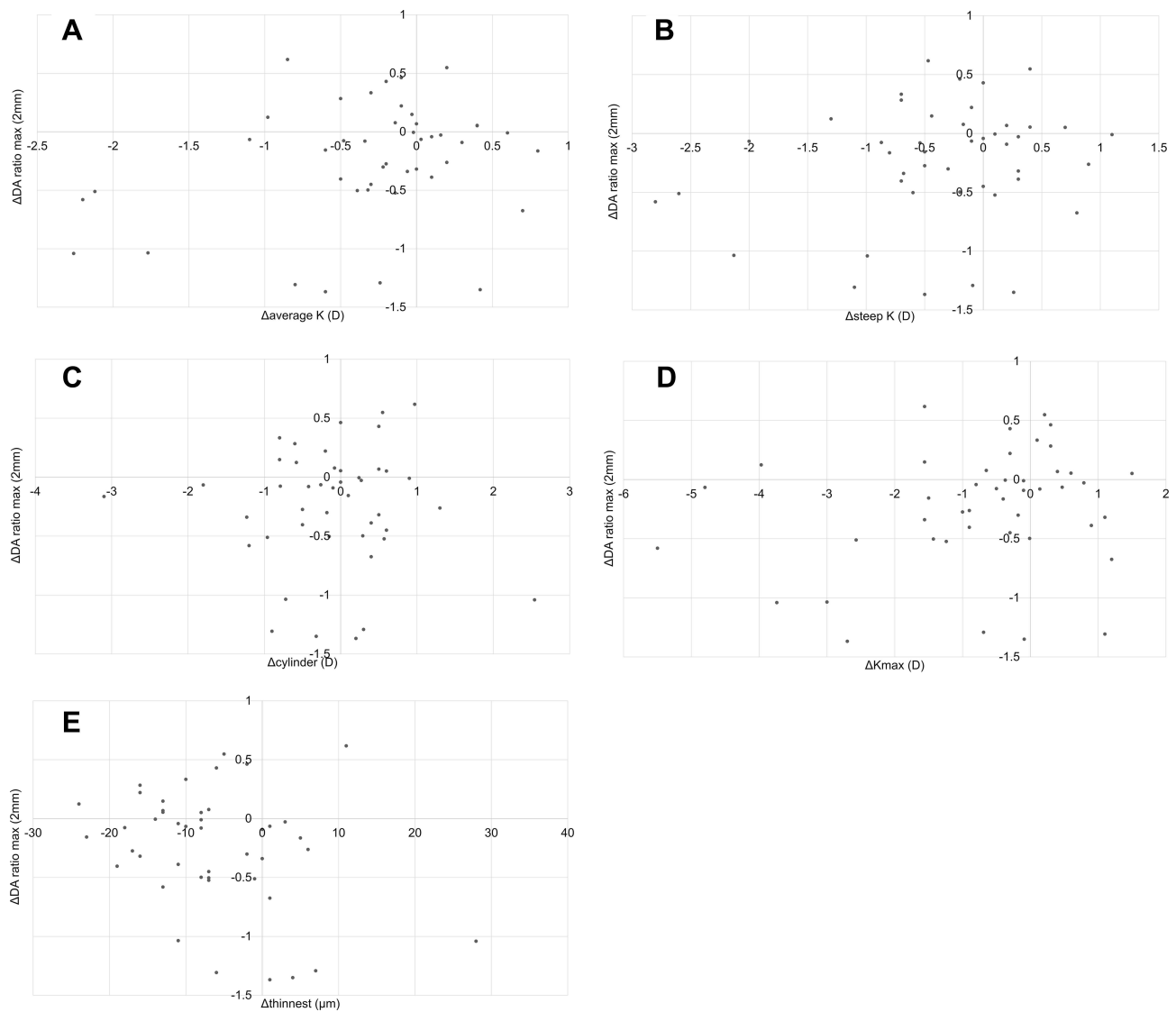
Figure 4 Correlation between each anterior segment optical coherence tomography (AS-OCT) parameter change and ΔDA ratio max (2 mm). No significant correlation was found between the change in each AS-OCT parameter and Δ deformation amplitude (DA) ratio max (2 mm). ((**A**) Δaverage K, R=0.228, p=0.137) ((**B**) Δsteep K, R=0.196, p=0.201) ((**C**) Δcylinder, R=0.075, p=0.628) ((**D**) Δ maximum keratometry [Kmax], R=0.216, p=0.159) ((**E**) Δthinnest, R=−0.265, p=0.083).

Many studies have reported changes in corneal biomechanical properties after CXL.[14,15,38–40] Furthermore, studies using the Schiøtz tonometer have reported that the lower the corneal stiffness before CXL, the greater the improvement in corneal stiffness after CXL.[41] Future studies using SBT are needed to determine whether the effect of CXL is related to corneal stiffness before CXL surgery.

There is a demarcation line formed in the corneal stroma after CXL as a criterion for determining the effect of CXL. It is believed that the deeper the demarcation line, the stronger is the effect of CXL.[42] However, according to a study using SBT, the depth of the demarcation line and the effect of CXL are unrelated.[15] Further studies should be performed to reveal the relationship between the CXL effect and the demarcation line in the future.

There are several limitations to our study. First, the current study was conducted retrospectively. We used data from 3 months after surgery, when there were few cases of dropout during follow-up. Therefore, there is a possibility of selection bias occurring. Furthermore, the current study evaluated the early outcomes after surgery. C-CXL has been reported to be stable from 1 month to 1 year after surgery.[43] Therefore, it is necessary to observe the changes in corneal shape over the long term in future studies.
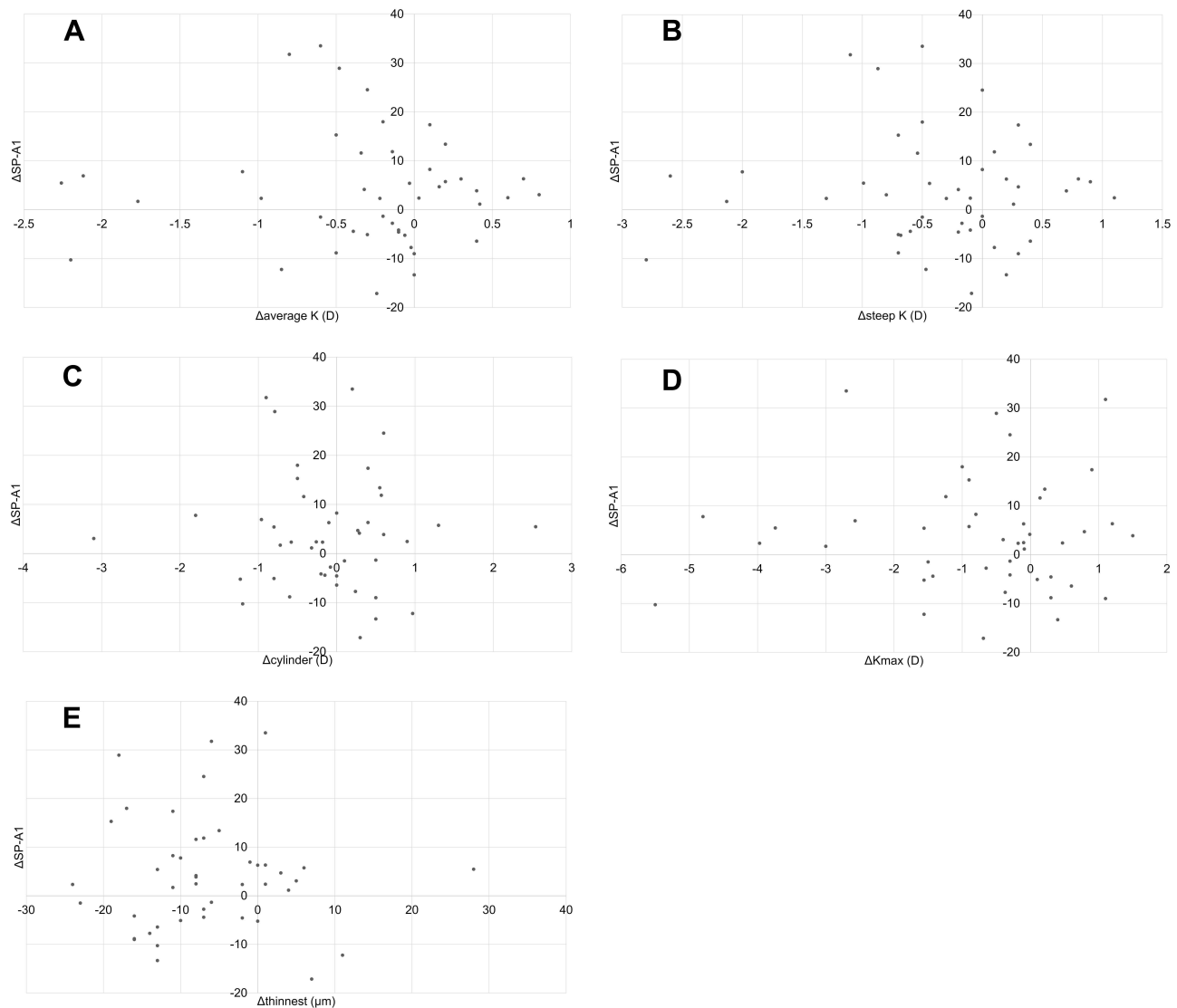
Figure 5 Correlation between each anterior segment optical coherence tomography (AS-OCT) parameter change and Δ stiffness parameter at applanation 1 (SP-A1). No significant correlation was found between the change in each AS-OCT parameter and ΔSP-A1. ((**A**) Δaverage K, R=−0.030, p=0.848) ((**B**) Δsteep K, R=−0.038, p=0.805) ((**C**) Δcylinder, R=−0.018, p=0.905) ((**D**) ΔKmax, R=−0.028, p=0.858) ((**E**) Δthinnest, R=0.47, p=0.762).

Furthermore, in the current study, only C-CXL was evaluated. C-CXL irradiates the cornea with ultraviolet light of different energies. Therefore, it is considered that the effect of corneal cross-linking can be obtained more strongly in the weaker part of the cornea. Therefore, our results may not apply to other methods of CXL. In the future, comparisons between multiple CXL methods will also be needed.

In this study, the parameters preoperative and postoperative CXL were evaluated, but it is important to predict the magnitude of the effect of CXL preoperative the procedure, which will be useful in determining the indication for CXL surgery.

Conclusions

Therefore, age, ΔIOP, Δaverage k, and Δthinnest were associated with the changes in the SBT parameters following C-CXL, which may be useful in determining the effectiveness of CXL.
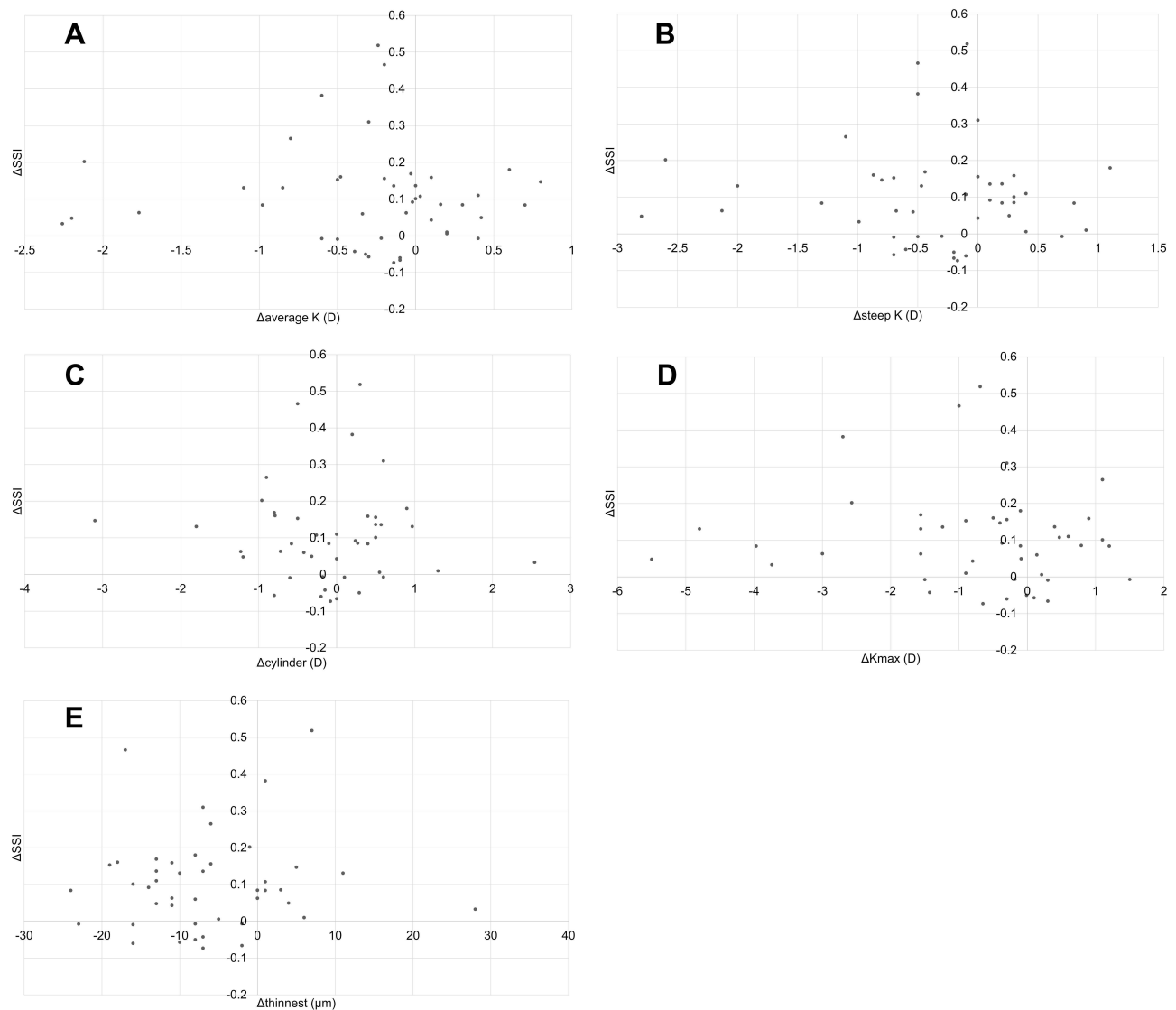
Figure 6 Correlation between each anterior segment optical coherence tomography (AS-OCT) parameter change and Δ stress-strain index (SSI). No significant correlation was found between the change in each AS-OCT parameter and ΔSSI. ((**A**) Δaverage K, R=−0.036, p=0.818) ((**B**) Δsteep K, R=−0.022, p=0.888) ((**C**) Δcylinder, R=−0.017, p=0.913) ((**D**) Δ maximum keratometry [Kmax], R=−0.111, p=0.474) ((**E**) Δthinnest, R=0.38, p=0.806).

Abbreviations

A-CXL, accelerated corneal crosslinking; average K, average keratometry; bIOP, biomechanically corrected intraocular pressure; C-CXL, customized corneal crosslinking; CDVA, corrected distance visual acuity; CXL, corneal crosslinking; DA, deformation amplitude; IOP, intraocular pressure; Kmax, maximum keratometry; NCT, non-contact tonometer; ORA, ocular response analyzer; RGP, rigid gas permeable; SBT, Scheimpflug-based tonometer; SP-A1, Stiffness parameter at applanation 1; SSI, Stress–Strain Index; Steep K, steep keratometry; UDVA, uncorrected distance visual acuity; UV, ultraviolet.

Data Sharing Statement

All data generated or analyzed during this study are included in this article. Further enquiries can be directed to the corresponding author.

Study Approval Statement

This retrospective study was approved by the Institutional Review Board of the Nagoya Eye Clinic (2021–47). The study was performed in accordance with the tenets of the Declaration of Helsinki.

Consent to Participate Statement

An opt-out method was approved, and the need for obtaining written informed consent was waived.

Author Contributions

All authors made a significant contribution to the work reported, including either the conception, study design, execution, acquisition of data, analysis, and interpretation, or all these areas; took part in drafting, revising or critically reviewing the article; gave final approval of the version to be published; have agreed on the journal to which the article has been submitted; and agree to be accountable for all aspects of the work.

Disclosure

Mr. Nishida has no commercial interests to disclose. Dr. Kojima reports receiving personal fees from Staar Surgical, Santen Pharmaceutical, Otsuka Pharmaceutical, and Alcon Japan, outside of the submitted work. Dr. Kojima also has a patent (2019-045345) licensed to Takashi Kojima. Mr. Kataoka, Mr. Isogai, and Dr. Yoshida have no commercial interests to disclose. Dr. Nakamura reports receiving personal fees from Staar Surgical, Santen Pharmaceutical, Otsuka Pharmaceutical, Carl Zeiss Meditec, and Johnson & Johnson, outside the submitted work. The authors report no other conflicts of interest in this work.

References

1. Krachmer JH, Feder RS, Belin MW. Keratoconus and related noninflammatory corneal thinning disorders. *Surv Ophthalmol*. 1984;28:293–322. doi:10.1016/0039-6257(84)90094-8
2. Chatzis N, Hafezi F. Progression of keratoconus and efficacy of pediatric [corrected] corneal collagen cross-linking in children and adolescents. *J Refract Surg*. 2012;28:753–758. doi:10.3928/1081597X-20121011-01
3. Elder MJ. Leber congenital amaurosis and its association with keratoconus and keratoglobus. *J Pediatr Ophthalmol Strabismus*. 1994;31:38–40. doi:10.3928/0191-3913-19940101-08
4. Wollensak G, Spoerl E, Seiler T. Riboflavin/ultraviolet-a-induced collagen crosslinking for the treatment of keratoconus. *Am J Ophthalmol*. 2003;135:620–627. doi:10.1016/s0002-9394(02)02220-1
5. Hafezi F, Mrochen M, Iseli HP, et al. Collagen crosslinking with ultraviolet-A and hypoosmolar riboflavin solution in thin corneas. *J Cataract Refract Surg*. 2009;35:621–624. doi:10.1016/j.jcrs.2008.10.060
6. Gkika M, Labiris G, Kozobolis V. Corneal collagen cross-linking using riboflavin and ultraviolet-A irradiation: a review of clinical and experimental studies. *Int Ophthalmol*. 2011;31:309–319. doi:10.1007/s10792-011-9460-x
7. Kolli S, Aslanides IM. Safety and efficacy of collagen crosslinking for the treatment of keratoconus. *Expert Opin Drug Saf*. 2010;9:949–957. doi:10.1517/14740338.2010.495117
8. Raiskup F, Theuring A, Pillunat LE, et al. Corneal collagen crosslinking with riboflavin and ultraviolet-A light in progressive keratoconus: ten-year results. *J Cataract Refract Surg*. 2015;41:41–46. doi:10.1016/j.jcrs.2014.09.033
9. Raiskup-Wolf F, Hoyer A, Spoerl E, et al. Collagen crosslinking with riboflavin and ultraviolet-A light in keratoconus: long-term results. *J Cataract Refract Surg*. 2008;34:796–801. doi:10.1016/j.jcrs.2007.12.039
10. Schindl A, Rosado-Schlosser B, Trautinger F. Reciprocity regulation in photobiology. An overview. *Hautarzt*. 2001;52:779–785. doi:10.1007/s001050170065
11. Pinelli R. BAK: a better alternative to epithelium removal in cross linking. *Ophthalmol Times Eur*. 2006;2:36–38.
12. Scarcelli G, Besner S, Pineda R, et al. Biomechanical characterization of keratoconus corneas ex vivo with Brillouin microscopy. *Invest Ophthalmol Vis Sci*. 2014;55:4490–4495. doi:10.1167/iovs.14-14450
13. Seiler TG, Fischinger I, Koller T, Zapp D, Frueh BE, Seiler T. Customized corneal cross-linking: one-year results. *Am J Ophthalmol*. 2016;166:14–21. doi:10.1016/j.ajo.2016.02.029
14. Nishida T, Kojima T, Kataoka T, et al. Comparison of corneal biomechanical properties and corneal tomography between customized and accelerated corneal crosslinking in eyes with keratoconus. *Cornea*. 2021;40:851–858. doi:10.1097/ICO.0000000000002572
15. Vinciguerra R, Tzamalis A, Romano V, et al. Assessment of the association between in vivo corneal biomechanical changes after corneal cross-linking and depth of demarcation line. *J Refract Surg*. 2019;35:202–206. doi:10.3928/1081597X-20190124-01
16. Uzel MM, Koc M, Can C, et al. Effect of accelerated corneal crosslinking on ocular response analyzer waveform-derived parameters in progressive keratoconus. *Arq Bras Oftalmol*. 2019;82:18–24. doi:10.5935/0004-2749.20190003

17. Hallahan KM, Sinha Roy A, Ambrosio R Jr, et al. Discriminant value of custom ocular response analyzer waveform derivatives in keratoconus. *Ophthalmology*. 2014;121:459–468. doi:10.1016/j.ophtha.2013.09.013

18. Wu Y, Li XL, Yang SL, et al. [Examination and discriminant analysis of corneal biomechanics with CorVis ST in keratoconus and subclinical keratoconus]. *Beijing Da Xue Xue Bao Yi Xue Ban*. 2019;51:881–886. Chinese.

19. Ren S, Xu L, Fan Q, et al. Accuracy of new Corvis ST parameters for detecting subclinical and clinical keratoconus eyes in a Chinese population. *Sci Rep*. 2021;11:4962. doi:10.1038/s41598-021-84370-y

20. Elham R, Jafarzadehpur E, Hashemi H, et al. Keratoconus diagnosis using Corvis ST measured biomechanical parameters. *J Curr Ophthalmol*. 2017;29:175–181. PMID: 28913507; PMCID: PMC5587249. doi:10.1016/j.joco.2017.05.002

21. Zhao Y, Shen Y, Yan Z, et al. Relationship among corneal stiffness, thickness, and biomechanical parameters measured by corvis ST, pentacam and ORA in keratoconus. *Front Physiol*. 2019;10:740. PMID: 31263429; PMCID: PMC6585623. doi:10.3389/fphys.2019.00740

22. Koh S, Inoue R, Maeda N, et al. Corneal tomographic changes during corneal rigid gas-permeable contact lens wear in keratoconic eyes. *Br J Ophthalmol*. 2022;106:197–202. doi:10.1136/bjophthalmol-2020-317057

23. Joda AA, Shervin MM, Kook D, et al. Development and validation of a correction equation for Corvis tonometry. *Comput Methods Biomech Biomed Engin*. 2016;19:943–953. doi:10.1080/10255842.2015.1077515

24. Yang K, Xu L, Fan Q, et al. Repeatability and comparison of new Corvis ST parameters in normal and keratoconus eyes. *Sci Rep*. 2019;9(1):15379. doi:10.1038/s41598-019-51502-4

25. Roberts CJ, Mahmoud AM, Bons JP, et al. Introduction of two novel stiffness parameters and interpretation of air puff-induced biomechanical deformation parameters with a dynamic Scheimpflug analyzer. *J Refract Surg*. 2017;33:266–273. doi:10.3928/1081597X-20161221-03

26. Eliasy A, Chen KJ, Vinciguerra R, et al. Determination of corneal biomechanical behavior in-vivo for healthy eyes using CorVis ST tonometry: stress–strain index. *Front Bioeng Biotechnol*. 2019;7:105. doi:10.3389/fbioe.2019.00105

27. Liu G, Rong H, Pei R, et al. Age distribution and associated factors of cornea biomechanical parameter stress-strain index in Chinese healthy population. *BMC Ophthalmol*. 2020;20:436. PMID: 33143686; PMCID: PMC7607623. doi:10.1186/s12886-020-01704-6

28. Zhao W, Shen Y, Jian W, et al. Comparison of corneal biomechanical properties between post-LASIK ectasia and primary keratoconus. *J Ophthalmol*. 2020;2020:5291485. doi:10.1155/2020/5291485

29. Tiveron MC Jr, Pena CRK, Hida RY, et al. Topographic outcomes after corneal collagen crosslinking in progressive keratoconus: 1-year follow-up. *Arq Bras Oftalmol*. 2017;80:93–96. doi:10.5935/0004-2749.20170023

30. Soeters N, van der Valk R, Tahzib NG. Corneal cross-linking for treatment of progressive keratoconus in various age groups. *J Refract Surg*. 2014;30:454–460. PMID: 24892379. doi:10.3928/1081597X-20140527-03

31. Vinciguerra R, Romano MR, Camesasca FI, et al. Corneal cross-linking as a treatment for keratoconus: four-year morphologic and clinical outcomes with respect to patient age. *Ophthalmology*. 2013;120:908–916. PMID: 23290750. doi:10.1016/j.ophtha.2012.10.023

32. Grišević S, Gilevska F, Biščević A, et al. Cross-linking treatment for better visual acuity. *Med Glas*. 2020;17:123–128. doi:10.17392/1071-20

33. Godefrooij DA, Boom K, Soeters N, et al. Predictors for treatment outcomes after corneal crosslinking for keratoconus: a validation study. *Int Ophthalmol*. 2017;37:341–348. doi:10.1007/s10792-016-0262-z

34. Greenstein SA, Fry KL, Hersh PS. Effect of topographic cone location on outcomes of corneal collagen cross-linking for keratoconus and corneal ectasia. *J Refract Surg*. 2012;28:397–405. doi:10.3928/1081597X-20120518-02

35. Tian M, Ma P, Zhou W, et al. Outcomes of corneal crosslinking for central and paracentral keratoconus. *Medicine*. 2017;96:e6247. doi:10.1097/MD.0000000000006247

36. Liu J, Roberts CJ. Influence of corneal biomechanical properties on intraocular pressure measurement: quantitative analysis. *J Cataract Refract Surg*. 2005;31:146–155. doi:10.1016/j.jcrs.2004.09.031

37. Kasumovic SS, Mavija M, Kasumovic A, et al. Intraocular pressure measurements referring to the corneal thickness in keratoconic eyes after corneal crosslinking with riboflavin and ultraviolet A. *Med Arch*. 2015;69:334–338. doi:10.5455/medarh.2015.69.334-338

38. Jabbarvand M, Moravvej Z, Shahraki K, et al. Corneal biomechanical outcome of collagen cross-linking in keratoconic patients evaluated by Corvis ST. *Eur J Ophthalmol*. 2021;31:1577–1583. doi:10.1177/1120672120944798

39. Salouti R, Khalili MR, Zamani M, Ghoreyshi M, Nowroozzadeh MH. Assessment of the changes in corneal biomechanical properties after collagen cross-linking in patients with keratoconus. *J Curr Ophthalmol*. 2019;31:262–267. doi:10.1016/j.joco.2019.02.002

40. Hashemi H, Ambrósio R Jr, Vinciguerra R, et al. Two-year changes in corneal stiffness parameters after accelerated corneal cross-linking. *J Biomech*. 2019;93:209–212. doi:10.1016/j.jbiomech.2019.06.011

41. Tutchenko L, Patel S, Skovron M, et al. The effect of corneal crosslinking on the rigidity of the cornea estimated using a modified algorithm for the Schiøtz tonometer. *Indian J Ophthalmol*. 2021;69:1531–1536. PMID: 34011736; PMCID: PMC8302317. doi:10.4103/ijo.IJO_1820_20

42. Spadea L, Tonti E, Vingolo EM. Corneal stromal demarcation line after collagen cross-linking in corneal ectatic diseases: a review of the literature. *Clin Ophthalmol*. 2016;10:1803–1810. doi:10.2147/OPTH.S117372

43. Kamiya K, Kanayama S, Takahashi M, et al. Visual and topographic improvement with epithelium-on, oxygen-supplemented, customized corneal cross-linking for progressive keratoconus. *J Clin Med*. 2020;9:3222. doi:10.3390/jcm9103222